Linear Stability Analysis of Gas-Liquid Interface

J.-G. Lee* and L.-D. Chen†
University of Iowa, Iowa City, Iowa 52242

This paper extends the Rayleigh theory to study the interface instability of axisymmetric gas-liquid flows. The dispersion equations of cylindrical liquid sheets were derived and numerical solutions were obtained. Two families of instability curves were found; one for symmetric disturbances and the other for antisymmetric disturbances. Two limiting cases can be recovered from derived dispersion equations. The equation recovers the Rayleigh instability of round jets for symmetric disturbances and recovers the hollow jet or submerged jet instability for antisymmetric disturbances. Effects due to ambient fluid density and ambient fluid velocity on liquid-sheet instabilities were examined.

Nomenclature

a = inner jet radius, m
b = outer jet radius, m
D = density ratio between the gas and liquid, ρ_g/ρ
I_0, I_1 = modified Bessel functions of the first kind of order 0 and 1, respectively
K_0, K_1 = modified Bessel functions of the second kind of order 0 and 1, respectively
k = disturbance wave number, $2\pi/\lambda$, 1/m
L = characteristic length
P = mean pressure
p = pressure fluctuation due to disturbances
$\hat{p}$ = instantaneous pressure
r = coordinate in radial direction
t = time, s
U = mean velocity of the liquid phase, m/s
U_j = relative velocity with respect to the coordinate moving with the liquid phase ($j = a,b$)
u = disturbance velocity, m/s
$\hat{u}$ = instantaneous velocity, m/s
We = Weber number, $\rho U^2/\sigma$
z = coordinate in axial direction
α = disturbance growth rate, rad/s
γ = parameter of Bessel functions, kr, where $r = a$ or b
γ_1 = parameter of Bessel functions, lr, where $l^2 = k^2 + \alpha/\nu$ and $r = a$ or b
η = disturbance expression, $Re\,[\eta_o \exp(ikz + \alpha t)]$
η_o = initial amplitude of disturbance
λ = wavelength of disturbance, m
μ = liquid-phase dynamic viscosity
ν = liquid-phase kinematic viscosity, μ/ρ
ρ = liquid-phase density, kg/m^3
σ = interface surface tension, N/m
τ = initial disturbance amplitude ratio
ω = dimensionless disturbance growth, $\alpha/\sqrt{\sigma/\rho L^3}$

Subscripts

a = quantity of the fluid inside the liquid sheet
b = quantity of the fluid outside the liquid sheet
g = gas phase
r = radial component
z = axial component

Introduction

GAS-LIQUID two-phase flow is common to practical combustion systems. Some examples are spray atomization of propulsion systems[1] and submerged jets of liquid-metal combustion.[2] One intrinsic feature of these processes is the existence of spatial and temporal periodicity of the flow. Although the Rayleigh stability theory[3] has been extended to the studies of liquid sheet breakup, e.g., pressure atomization,[4,5] similar analyses for air-assisted atomization and submerged jets were not available. The purpose of this investigation is to extend the Rayleigh theory to study the interface instability of axisymmetric gas-liquid flows. The present analysis differs from earlier theories in that both the inner and outer interfaces are subject to the gas flow. The theory is also shown to return to simplified conditions such as the Rayleigh[3] and hollow jet[6] (submerged jet) instabilities when proper boundary conditions are specified. The objective of this paper is to present a stability theory for axisymmetric gas-liquid flows and the results of the analysis.

Three regimes have been identified for air-assisted atomization[7]; namely, the Rayleigh, intermittent, and atomization regimes. The three regimes identified by Lee and Chen[7] are qualitatively similar to Rayleigh, wind-induced, and atomization regimes of pressure atomization identified by Reitz and Bracco.[4,5] Typical visualization of the atomization process studied in Ref. 7 is illustrated in Fig. 1, in which a large concentric nozzle was used. In the experiments, air was fed through the central jet and water through the annular jet. The inside diameters of the inner and outer tubes are, respectively, 9.5 and 22.2 mm, and the tube wall thickness is 1.6 mm. The length of the tube is 419 mm for the inner tube and 444 mm for the outer tube. Detailed description of the nozzle can be found in Ref. 7. At low airflow rates, periodic bubble formation was observed. This bubble-formation regime was termed the Rayleigh regime due to the similarity between the bubble formation and the droplet formation of low-velocity liquid jets. The bubble size was found to be about twice of the outer tube (annular jet) diameter and the formation frequency was typically in the range 5–30 Hz for the conditions examined in Ref. 7. As the airflow rate was increased, the spacing between bubbles decreased, and the bubble shape was distorted. This regime was termed the intermittent regime.[7] With further increase the airflow rate, small

Received Nov. 20, 1989; presented as Paper 90-0446 at the AIAA 28th Aerospace Sciences Meeting, Reno, NV, Jan. 8–11, 1990; revision received Nov. 26, 1990; accepted for publication Dec. 3, 1990.

*Graduate Assistant, Department of Mechanical Engineering; currently Associate Research Engineer, CFD Research Corp., 3325D Triana Boulevard, Huntsville, AL 35805.
†Associate Professor, Department of Mechanical Engineering. Member AIAA.

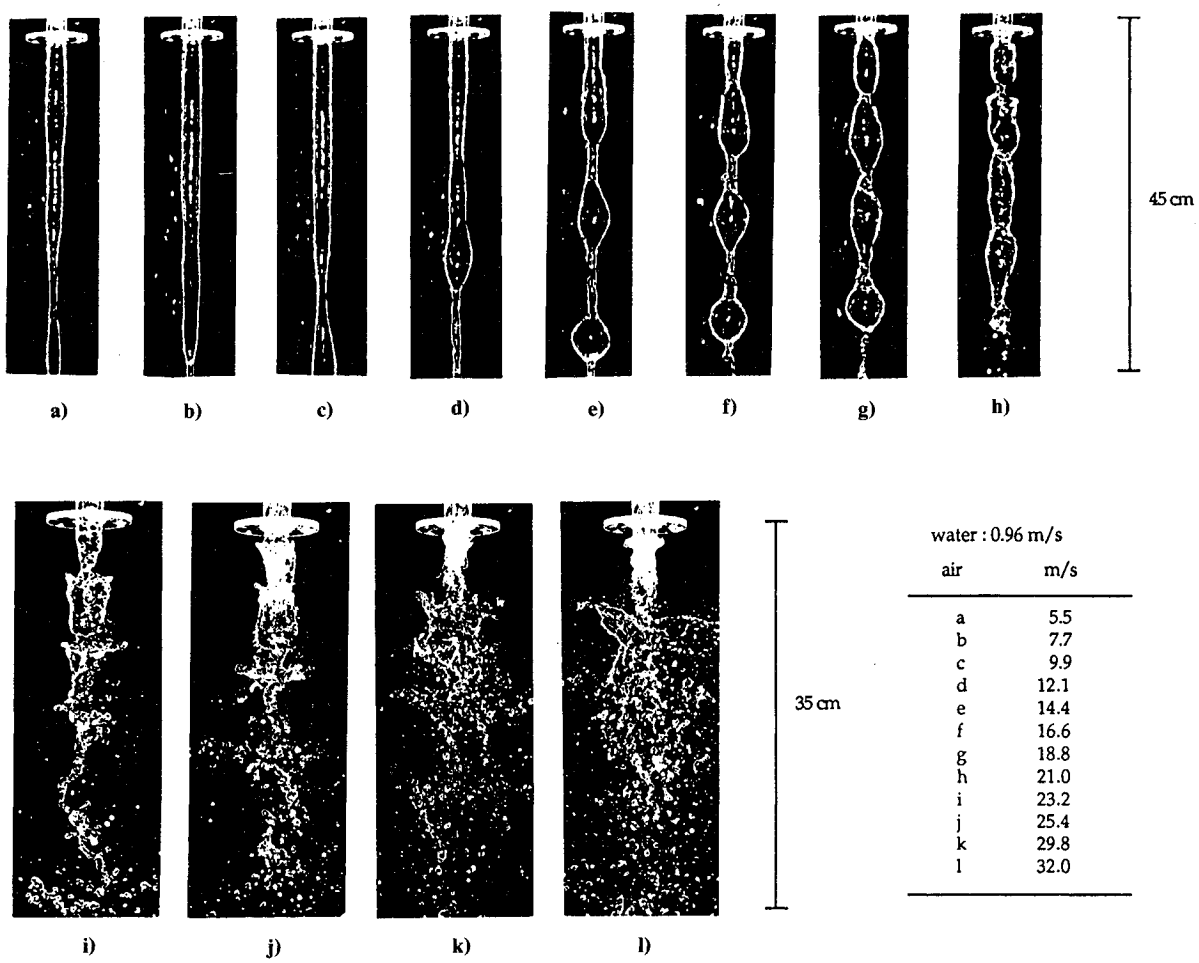

Fig. 1 Flow characteristics of annular jets (water velocity = 0.96 m/s).

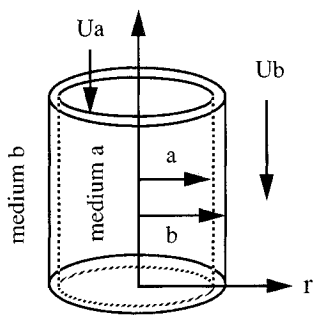

Fig. 2 Coordinates of the cylindrical liquid sheet.

liquid drops were formed near the nozzle exit and the flow regime was named the atomization regime.

The stability theory developed for cylindrical liquid sheets subject to gas flows at both inner and outer interfaces is applied to the atomization process illustrated in Fig. 1. It is hoped that a better understanding of the complex spray phenomenon can be obtained from the analysis based on the first principles of fluid mechanics, which in turn can establish a solid scientific base to explore effective methods to improve system performance.

Linear Instability Analysis

The Rayleigh[3] stability theory assumes no coflowing gas flow around the liquid jet; the present analysis allows for coflowing gas flows at both sides of the cylindrical liquid sheet, extending the work of Meyer and Weihs.[8] The major assumptions employed in analysis include the axisymmetry of the flow, the incompressible flow assumption for both phases, the inviscid flow assumption of the gas phase, and small disturbance at the gas-liquid interface. Following the coordinate system shown in Fig. 2, the disturbance equation at the liquid surface becomes

$$\eta = Re\,[\eta_{oj} \exp(ikz + \alpha t)] \tag{1}$$

where η_{oj} is the amplitude of the disturbance, k is the real wave number, and α is the complex circular frequency [α = Re(α) + i Im(α)]. In the context of stability analysis, the disturbance will amplify if Re(α) is a positive number and will decay if Re(α) is a negative number.

The instantaneous velocity ($\hat{u}_z$ and $\hat{u}_r$) and pressure $\hat{p}$ can be decomposed into two components, the mean and disturbance quantities:

$$\hat{u}_z = U + u_z \tag{2}$$

$$\hat{u}_r = u_r \tag{3}$$

$$\hat{p} = P + p \tag{4}$$

where u_z, u_r, and p are the disturbance velocities and pressure. Substituting the above quantities into the momentum equation and neglecting the nonlinear terms, one obtains linearized disturbance equations. With the coordinate system moving with the liquid surface at the same velocity U, the disturbance equations assume the following form:

$$\nabla \cdot u = 0, \qquad \nabla \cdot u_j = 0, \qquad j = a, b \tag{5}$$

$$\frac{\partial u}{\partial t} = \frac{1}{\rho}\nabla p + \frac{\mu}{\rho}\nabla^2 u \qquad \text{(liquid phase)} \qquad (6)$$

$$\frac{\partial u_b}{\partial t} + U_b\frac{\partial u_b}{\partial z} = -\frac{1}{\rho_b}\nabla p_b \qquad \text{(external medium)} \qquad (7)$$

$$\frac{\partial u_a}{\partial t} + U_a\frac{\partial u_a}{\partial z} = -\frac{1}{\rho_a}\nabla p_a \qquad \text{(internal medium)} \qquad (8)$$

The boundary conditions for the above equations require that the kinematic and dynamic equilibria be satisfied at the inner and outer interfaces. The kinematic equilibrium states that

$$u_r = \frac{\partial \eta_j}{\partial t}, \qquad (j = a, b; \text{ liquid phase}) \qquad (9)$$

$$u_{rj} = \frac{\partial \eta_j}{\partial t} + U_j\frac{\partial \eta_j}{\partial z}, \qquad (j = a, b; \text{ gas phase}) \qquad (10)$$

The dynamic equilibrium requires the balance of shear and normal stresses across the interface. Following Sterling and Sleicher,[9] the shear stress is assumed to vanish at the interface, yielding

$$\frac{\partial u_z}{\partial r} + U_j\frac{\partial u_r}{\partial z} = 0 \qquad (11)$$

and the normal stress is balanced by the pressure and surface tension:

$$-p + 2\mu\frac{\partial u_r}{\partial r} = -p_a + p_\sigma, \qquad \text{(interface } a\text{)} \qquad (12)$$

$$-p + 2\mu\frac{\partial u_r}{\partial r} = -p_b - p_\sigma, \qquad \text{(interface } b\text{)} \qquad (13)$$

In the above equations, p, p_a and p_b are, respectively, the pressures of the liquid phase, the gas medium a, and the gas medium b, and p_σ is due to the surface tension at the interface which can be determined from

$$p_\sigma = -\frac{\sigma}{r^2}\left(\eta_j + r^2\frac{\partial^2\eta_j}{\partial z^2}\right), \qquad j = a,b \qquad (14)$$

The dispersion equations or the disturbance growth rate equations are derived from solving the governing equations, Eqs. (5–8), at the boundary conditions specified by Eqs. (9–13). The obtained growth rate equation at the interface a is

$$\left[\frac{1}{M(\gamma_a,\gamma_b)}\left(\frac{\tau}{\gamma_a} - X(\gamma_a,\gamma_b)\right) - D_a\frac{I_0(\gamma_a)}{I_1(\gamma_a)}\right]\alpha^2 + 2\left[\frac{iD_aU_a\gamma_a}{a}\frac{I_0(\gamma_a)}{I_1(\gamma_a)} + \left(\frac{\nu\gamma_a}{a^2}\right) \times \left(\frac{2\{\tau - \gamma_a X(\gamma_a,\gamma_b)\}}{M(\gamma_a,\gamma_b)} - 1\right)\right]\alpha = -\frac{\sigma\gamma_a}{\rho a^3}(1-\gamma_a^2) - \frac{D_aU_a^2\gamma_a^2}{a^2}\frac{I_0(\gamma_a)}{I_1(\gamma_a)} - \left(\frac{4\nu^2\gamma_a^3}{a^4}\right)\left(\frac{\tau - \gamma_a X(\gamma_a,\gamma_b)}{M(\gamma_a,\gamma_b)} + \frac{\tau - \gamma_{1a}X(\gamma_{1a},\gamma_{1b})}{M(\gamma_{1b},\gamma_{1a})}\right) \qquad (15)$$

and that at the interface b is

$$\left[\frac{1}{M(\gamma_a,\gamma_b)}\left(X(\gamma_b,\gamma_a) - \frac{1}{\tau\gamma_b}\right) - D_b\frac{K_0(\gamma_b)}{K_1(\gamma_b)}\right]\alpha^2 + 2\left[\frac{iD_bU_b\gamma_b}{b}\frac{K_0(\gamma_b)}{K_1(\gamma_b)} + \left(\frac{\nu\gamma_b}{b^2}\right) \times \left(\frac{2\{\gamma_b X(\gamma_b,\gamma_a) - (1/\tau)\}}{M(\gamma_a,\gamma_b)} - 1\right)\right]\alpha = \frac{\sigma\gamma_b}{\rho b^3}(1-\gamma_b^2) + \frac{D_bU_b^2\gamma_b^2}{b^2}\frac{K_0(\gamma_b)}{K_1(\gamma_b)} - \left(\frac{4\nu^2\gamma_b^3}{b^4}\right)\left(\frac{\gamma_b X(\gamma_b,\gamma_a) - (1/\tau)}{M(\gamma_a,\gamma_b)} + \frac{\gamma_{1b}X(\gamma_{1b},\gamma_{1a}) - (1/\tau)}{M(\gamma_{1b},\gamma_{1a})}\right) \qquad (16)$$

where $I_m(\gamma)$ and $K_n(\gamma)$ are the Bessel functions of the first and second kinds, order m and n respectively, and

$$D_a = \rho_a/\rho, \quad D_b = \rho_b/\rho, \quad \gamma_a = ka, \quad \gamma_b = kb$$

$$\gamma_{1a} = la, \quad \gamma_{1b} = lb, \quad l^2 = k^2 + (\alpha/\nu)$$

$$\tau = \eta_{ob}/\eta_{oa}, \quad s = 1/\tau$$

$$M(x_1,x_2) = K_1(x_1)I_1(x_2) - K_1(x_2)I_1(x_1)$$

$$X(x_1,x_2) = K_1(x_2)I_0(x_1) + K_0(x_1)I_1(x_2)$$

Equations (15) and (16) are the generalized dispersion equations at the interfaces a and b. The growth rate equations, i.e., Eqs. (15) and (16), are quite complex, precluding the use of analytic solutions; however, assuming low viscosity ($\nu \ll 1$) and same wave number k and growth rate α for both interfaces, Eqs. (15) and (16) can be combined into one equation. This was accomplished by eliminating the ratio of initial disturbance amplitudes τ from the above equations, yielding

$$(GH - 1/M^2\gamma_a\gamma_b)\alpha^4 + (GD - BH)\alpha^3 + (HC - BD - GE)\alpha^2 + (BE + CD)\alpha - CE = 0 \qquad (17)$$

where

$$B = 2i\frac{D_aU_a\gamma_a}{a}\frac{I_0(\gamma_a)}{I_1(\gamma_a)}$$

$$C = -\frac{\sigma\gamma_a}{\rho a^3}(1-\gamma_a^2) - \frac{D_aU_a^2\gamma_a^2}{a^2}\frac{I_0(\gamma_a)}{I_1(\gamma_a)}$$

$$D = 2i\frac{D_bU_b\gamma_b}{b}\frac{K_0(\gamma_b)}{K_1(\gamma_b)}$$

$$E = \frac{\sigma\gamma_b}{\rho b^3}(1-\gamma_b^2) + \frac{D_bU_b^2\gamma_b^2}{b^2}\frac{K_0(\gamma_b)}{K_1(\gamma_b)}$$

$$G = \frac{X(\gamma_a,\gamma_b)}{M(\gamma_a,\gamma_b)} + D_a\frac{I_0(\gamma_a)}{I_1(\gamma_a)}$$

$$H = \frac{X(\gamma_b,\gamma_a)}{M(\gamma_a,\gamma_b)} + D_b\frac{K_0(\gamma_b)}{K_1(\gamma_b)}$$

It is noted that Eq. (17) is similar to that obtained by Crapper et al.[10] The present study, however, can be subject to different

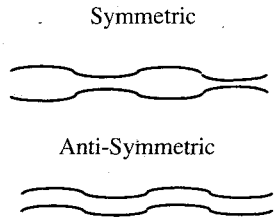

Fig. 3 Schematic of symmetric and antisymmetric disturbances of planar jets.

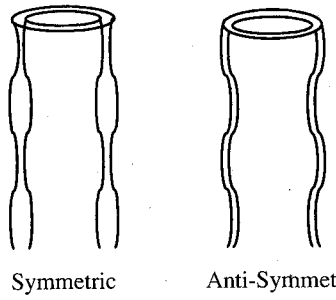

Fig. 4 Schematic of symmetric and antisymmetric disturbances of cylindrical liquid sheets.

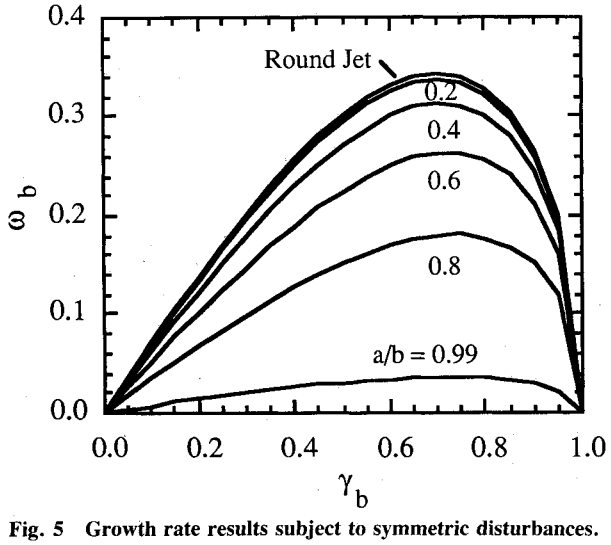

Fig. 5 Growth rate results subject to symmetric disturbances.

velocities at both inside and outside interfaces, which was not considered in Ref. 10.

Results and Discussion

Equations (15) and (16) can be simplified to recover earlier stability analyses of round liquid jets (Rayleigh stability) and hollow jets. Equation (17) can also be solved numerically and recovers earlier analyses. Two families of solutions were obtained from Eq (17). One has a positive initial amplitude ratio that recovers the instability equation of hollow jets and the other with a negative ratio recovers the instability equation of round jets. Previous studies[3,11] of planar jet instabilities also showed that there existed two families of solution; one corresponds to the negative initial amplitude ratio τ, and the other corresponds to the positive one. A negative τ for a planar jet can be interpreted as a symmetric or "varicose" disturbance, whereas a positive τ represents an antisymmetric or "sinuous" disturbance, e.g., see Fig. 3. For cylindrical sheets, similar definitions were employed as illustrated in Fig. 4.

Rayleigh Stability

Assuming an inviscid liquid with negligible effects from the surrounding fluids, i.e., $U_b = U_a = D_a = D_b = 0$, the Rayleigh instability equation of round jets can be recovered from the analysis. This was accomplished by introducing a disturbance at the outer interface and setting the ratio a/b and the disturbance at the inner interface both to zero. Equation (16) then recovers to the Rayleigh equation[3]:

$$\alpha^2 = (\sigma\gamma_b/\rho b^3)(1 - \gamma_b^2)\,[I_1(\gamma_b)/I_0(\gamma_b)] \qquad (18)$$

Instability can occur when α is a real number or γ_b is less than one. This condition corresponds to the instability due to long-wavelength disturbances. As for short-wavelength disturbances, Eq. (18) is reduced to

$$\alpha^2 = -\sigma k^3/\rho \qquad (19)$$

where α is an imaginary number and the disturbance will not amplify.

When the influence of the ambient fluid needs to be considered, for example, low-viscosity jets subject to short-wavelength disturbance, the growth rate equation at the interface b becomes

$$\alpha^2 = (\rho_b k^2 U_b^2 - \sigma k^3)/\rho \qquad (20)$$

The above equation, which recovers to that derived by Levich,[12] shows that the inclusion of U_b in the dispersion equation results in an unstable disturbance to otherwise stable situations when the interface is subject to a short-wavelength disturb-

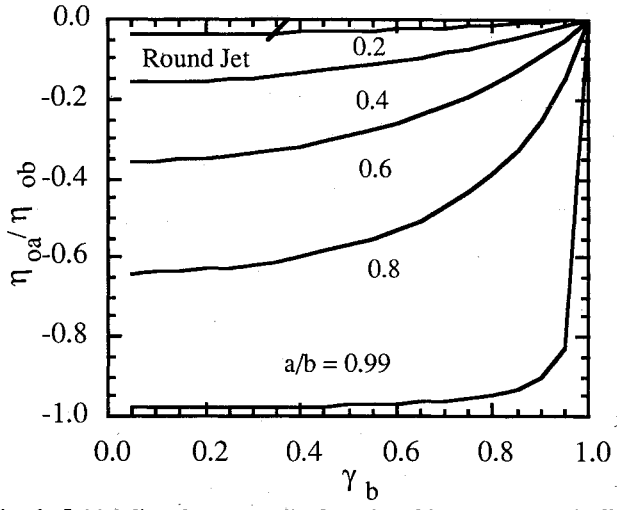

Fig. 6 Initial disturbance amplitude ratio subject to symmetric disturbances.

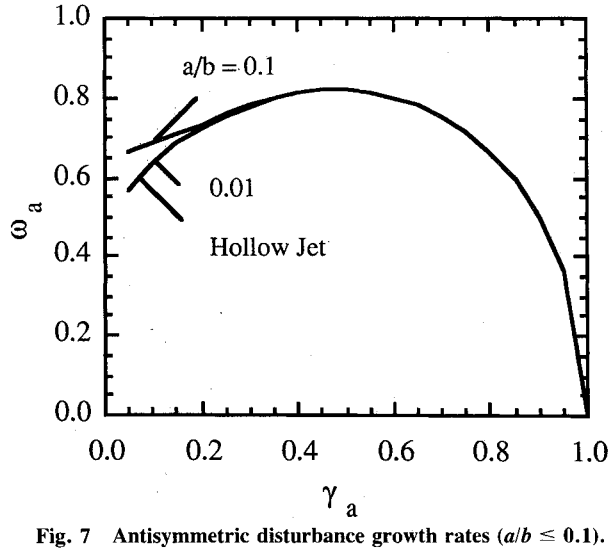

Fig. 7 Antisymmetric disturbance growth rates ($a/b \leq 0.1$).

ance. When α is a real number, an instability will occur and the disturbance amplitude will amplify.

The family of solutions due to symmetric disturbances (i.e., negative initial disturbance amplitude ratio) with the liquid sheet thickness as a parameter is shown in Fig. 5. In the figure, dimensionless growth rate ω_b [$= \alpha/(\rho b^3)^{0.5}$] was plotted against dimensionless wave number γ_b ($= kb$). When the thickness ratio a/b was decreased (i.e., a thicker liquid sheet), the growth rate was increased. When a/b approaches zero, the solution recovers to the round jet results. It should be noted that the liquid sheet is unstable when $0 < \gamma_b < 1$ but stable when $\gamma_b > 1$. The result shown in Fig. 5 is based on the solution of the initial disturbance amplitude ratio η_{oa}/η_{ob} as a function of γ_b at different a/b ratios, e.g., see Fig. 6. The disturbances at the inner and outer interfaces are 180 deg out of phase (symmetric) and the magnitude of η_{oa}/η_{ob} approached zero and $(a/b)^2$ as γ_b approaches zero and one, respectively. The magnitude of η_{oa}/η_{ob} decreases as a/b is decreased and is zero at the round liquid jet limit, i.e., $a/b = 0$.

Submerged Jets

When the outer radius becomes infinite while keeping the inner radius a finite value, the configuration then becomes a submerged gas jet in liquids or a hollow jet condition considered by Chandrasekhar.[6] The dispersion equation at this condition was obtained from Eq. (15) at the limit b approaching infinity:

$$\alpha^2 = \frac{\sigma\gamma_a}{\rho a^3}(1 - \gamma_a^2)\frac{K_1(\gamma_a)}{K_0(\gamma_a)} \tag{21}$$

The family of solutions due to antisymmetric disturbances, i.e., $\eta_{ob}/\eta_{oa} > 0$, with the liquid sheet thickness as a parameter was obtained from Eq. (17). The numerical solutions are summarized in Figs. 7 and 8 with dimensionless growth rate ω_a defined as $\alpha/(\rho a^3)^{0.5}$. The results showed that when the thickness ratio a/b approaches zero, the solution approaches that of a submerged jet or a hollow jet. In contrast to symmetric disturbances, the growth rate of antisymmetric disturbances increases as the liquid sheet thickness is decreased. The calculation is based on the solution of the initial disturbance amplitude ratio t as a function of γ_a at different thickness ratios a/b; cf. Fig. 9. Figure 9 shows that the disturbance at the inner and outer interfaces are in phase. The ratio η_{ob}/η_{oa} approaches zero and a/b as γ_a approaches one and zero, respectively, and it increases as a/b is increased.

Annular Jets

The annular jet can be considered as an approximation of the air-assisted atomization studied in Ref. 7. From the results

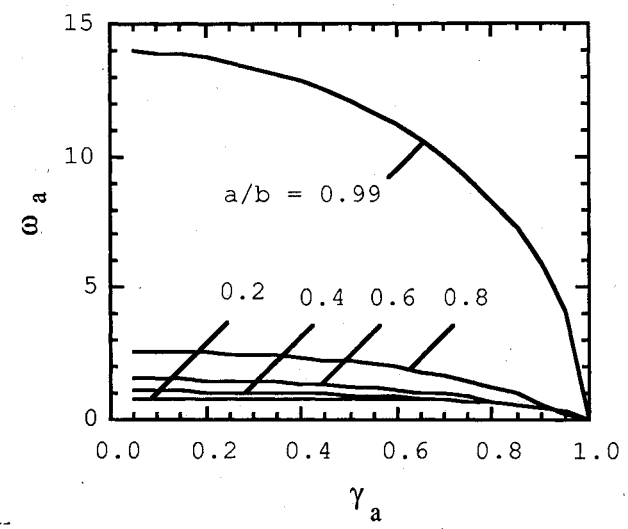

Fig. 8 Antisymmetric disturbance growth rates ($0.2 \leq a/b \leq 0.99$).

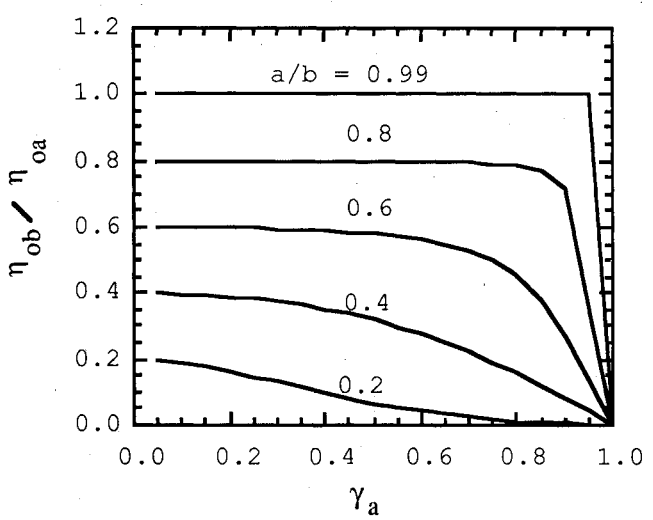

Fig. 9 Initial disturbance amplitude ratio subject to antisymmetric disturbances.

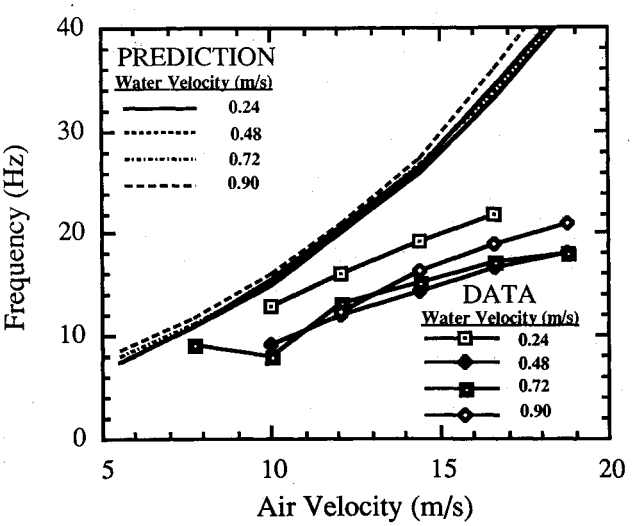

Fig. 10 Comparison between predicted and measured bubble-formation frequency at different test conditions (water velocity = 0.24, 0.48, 0.72, and 0.90 m/s).

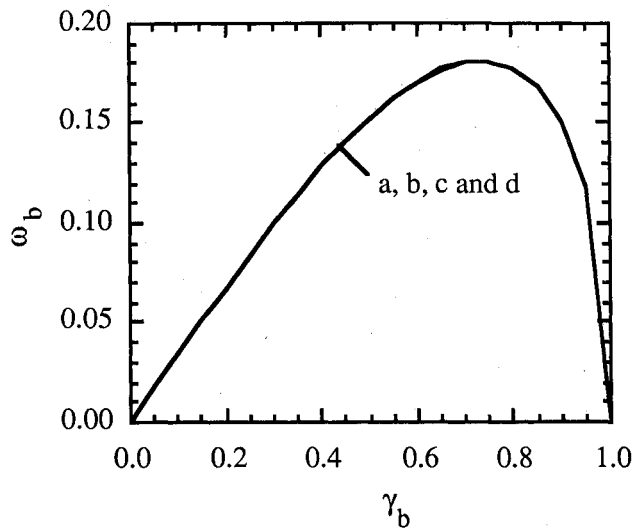

Fig. 11 Effect of air presence on symmetric disturbance. Case identification: a) no air; b) outer only; c) inner only; and d) both interface.

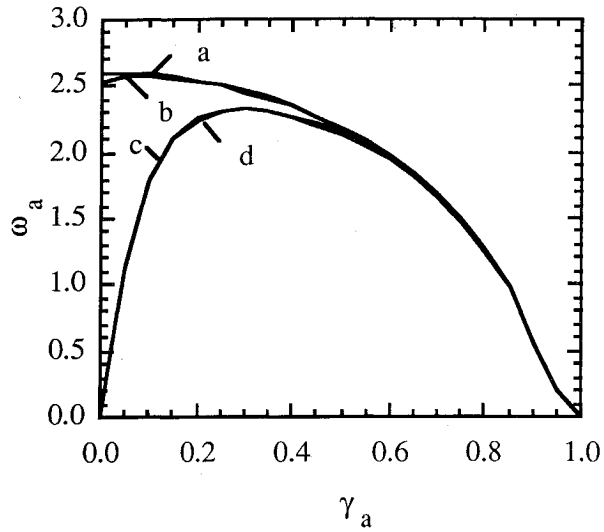

Fig. 12 Effect of air presence on antisymmetric disturbance. Case identification: a) no air; b) outer only; c) inner only; and d) both interface.

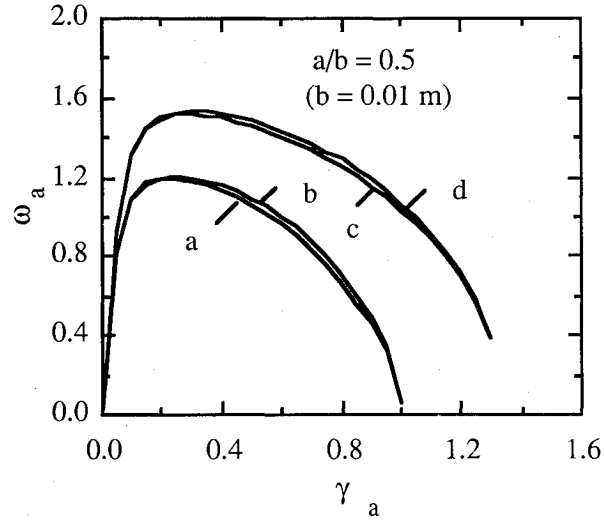

Fig. 13 Effects of air flow on growth rates of antisymmetric disturbances. Case identification: a) $U_a = U_b = 0$; b) $U_a = 0$ m/s, $U_b = 2$ m/s; c) $U_a = 2$ m/s, $U_b = 0$ m/s; and d) $U_a = U_b = 2$ m/s ($a/b = 0.5$).

shown earlier, it is clear that antisymmetric disturbances yield a higher growth rate than symmetric disturbances and that eventually the antisymmetric disturbance will dominate and lead to the breakup of liquid sheets. It is noted that the flow in the Rayleigh regime as identified in Fig. 1 exhibited the same curvature direction of the inner and outer interfaces, suggesting that the disturbances are in phase (or antisymmetric) at this condition—consistent with analysis. It is also due to an antisymmetric disturbance; periodic bubbles were formed.

Employing the growth rate equation, Eq. (17), the predicted bubble-formation frequency is evaluated and compared with the experimental measurements. The result is shown in Fig. 10. The results show that the prediction overestimates the bubble-formation frequency, especially when the air velocity is increased where the intermittent regime is approached. Nevertheless, the prediction using linear instability theory provides reasonable agreement with the measurement. More detailed discussion can be found in Ref. 13.

The effects on the growth rate due to the presence of air at the inner and outer interfaces are examined by solving Eq. (17). The results of symmetric and antisymmetric disturbances

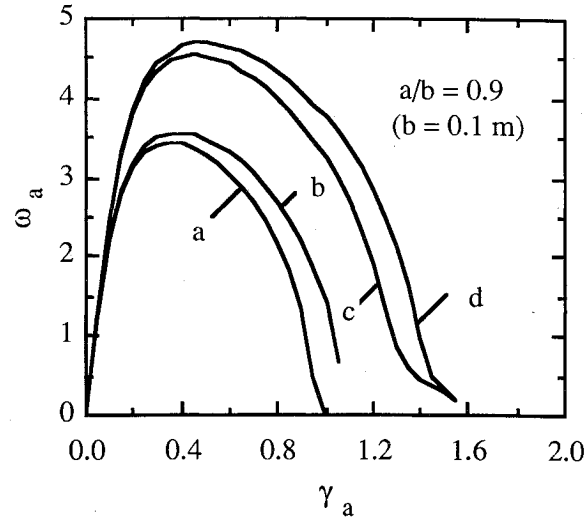

Fig. 14 Effects of airflow on growth rates of antisymmetric disturbances. Case identification: a) $U_a = U_b = 0$; b) $U_a = 0$ m/s, $U_b = 2$ m/s; c) $U_a = 2$ m/s, $U_b = 0$ m/s; and d) $U_a = U_b = 2$ m/s ($a/b = 0.9$).

are shown in Figs. 11 and 12, respectively. The presence of air does not have discernible effects on symmetric disturbances; however, it shifts the maximum growth rate to a larger wave number (or a shorter wavelength) for antisymmetric disturbances, which favors the bubble formation; cf. Fig. 12.

The effects of air velocity on the growth rates with two different thickness ratios and an outer radius b of 0.01 m are shown in Figs. 13 and 14 for $a/b = 0.5$ and 0.9, respectively. It should be noted that only antisymmetric disturbances were considered in Figs. 13 and 14 and that the 2 m/s air velocity employed in the computation is somewhat arbitrary, although it is a "typical" value of our flow conditions. The results presented in Figs. 13 and 14 showed that the growth rate increased as the thickness ratio was increased, or the liquid thickness is decreased, and that the inner fluid has a higher growth rate at comparable conditions. The viscosity effects neglected in Figs. 13 and 14 can be included when considering Eqs. (15) and (16). Further work is necessary to assess the viscosity effects.

Summary and Conclusions

A theoretical analysis based on linear stability theory was presented for cylindrical liquid sheets. The generalized dispersion equations or the growth rate equations can recover simplified conditions, including the Rayleigh equation[3] and the hollow jet solution[6] when pertinent assumptions and boundary conditions were applied. The dispersion equation was applied to the air-assisted atomization configuration studied in Ref. 7. The analytic results were also compared with the experimental measurements, and the comparison shows reasonable agreement. The analysis showed promising results for air-assisted atomization in terms of the effects due to the film thickness, air density, and velocity. The analysis also showed that the disturbance applied at the inner interface is a more effective way of atomization than that applied at outer interface. This observation, however, is yet to be verified by experiments. Work is in progress to characterize different atomization regimes observed in Ref. 7, to assess viscosity effects, and to examine the interface instabilities of submerged jets in a liquid bath.

Acknowledgment

This work was supported, in part, by the Air Force Wright Research and Development Center through Contract AFWAL F33615-84-C-2412/GC-1416-87-014.

References

[1]Lefebvre, A. H., *Gas Turbine Combustion*, McGraw-Hill, New York, 1983, pp. 357–461.

[2]Hughes, T. G., Smith, R. B., and Kiley, D. H., "Stored Chemical Energy Propulsion Systems for Underwater Applications," *Journal of Energy*, Vol. 7, No. 2, 1983, pp. 128–133.

[3]Rayleigh, L., *Theory of Sound*, Vol. 2, Dover, New York, 1945, pp. 351–365.

[4]Reitz, R. D., "Atomization and Other Breakup Regimes of a Liquid Jet," Ph.D. Thesis, Princeton Univ., Princeton, NJ, 1978.

[5]Reitz, R. D., and Bracco, F. V., "Mechanisms of Breakup of Round Liquid Jets," *Encyclopedia of Fluid Mechanics*, Vol. 3, edited by N. P. Cheremisinoff, Gulf, Houston, TX, 1986, pp. 233–249.

[6]Chandrasekhar, S., *Hydrodynamic and Hydromagnetic Stability*, Dover, New York, 1961, pp. 515–576.

[7]Lee, J. G., and Chen, L.-D., "Breakup of Cylindrical Liquid Sheets," *Proceedings of 1989 Spring Technical Meeting of the Central States Section of The Combustion Institute*, Dearborn, MI, April 30–May 3, The Combustion Inst., Pittsburgh, PA, 1989, pp. 307–312.

[8]Meyer, J., and Weihs, D., "Capillary Instability of an Annular Liquid Jet," *Journal of Fluid Mechanics*, Vol. 179, June 1987, pp. 531–545.

[9]Stirling, A. M., and Sleicher, C. A., "The Instability of Capillary Jets," *Journal of Fluid Mechanics*, Vol. 68, April 1975, pp. 477–495.

[10]Crapper, G. D., Dombrowski, N., and Pyott, G. A. D., "Kelvin-Holmhotz Wave Growth on Cylindrical Sheets," *Journal of Fluid Mechanics*, Vol. 68, April 1975, pp. 497–502.

[11]Lamb, H., *Hydrodynamics*, Dover, New York, 1945, pp. 374–375.

[12]Levich, V. G., *Physicochemical Hydrodynamics*, Prentice-Hall, Englewood Cliffs, NJ, 1962, pp. 591–668.

[13]Lee, J. G., "Breakup of Cylindrical Liquid Sheets," Ph.D. Thesis, Dept. of Mechanical Engineering, Univ. of Iowa, Iowa City, IA, 1990.